Buckling Support Structure for Automotive Interior Display

Sergey Shubin [a], Alyona Chubyuk [b], Nikolai Antipin [c]

a. Corning SAS, Finland, shubins@corning.com, shubinsn@gmail.com
b. Corning SAS, Finland, chubyuka2@corning.com
c. Corning SAS, Finland, antipinna@corning.com, antipinkolya@yandex.ru

Abstract

In this work, we propose a design concept for an automotive display support structure that improves glass performance in a headform impact test. The main idea is a bilinear response of the structure under head impact loading conditions: it has high stiffness at low loading magnitudes and significantly lower stiffness at high loading magnitudes. Such a bilinear response improves the cover glass performance in the headform impact test without losing display functionality. I.e., the display is still stiff for its regular use, but it has capability to smoothly absorbs kinetic energy of the headform. To achieve the bilinear response, we propose to use a structure that elastically buckles under high loads. The main advantage of this approach is that there is no residual deformation and no need to rebuild the structure after the impact. The concept is evaluated by finite element modelling using the LS-DYNA explicit solver and compared with a typical structure used in the industry.

Keywords

Interior automotive glass, display, headform impact, impact test, strengthened cover glass

Article Information

- Published by Glass Performance Days, on behalf of the author(s)
- Published as part of the Glass Performance Days Conference Proceedings, June 2025
- Editors: Jan Belis, Christian Louter & Marko Mökkönen

1. Introduction

Automotive interior displays are widely used in vehicles to provide information and control functions to the driver and passengers. Modern automotive interior displays can be touch screens, digital instrument clusters, head-up displays, or infotainment systems, offering a range of features to enhance the driving experience and convenience for the occupants. Glass used for automotive interior displays needs to meet several requirements to ensure functionality, safety, durability, and aesthetic appeal. Some typical requirements for glass used in automotive interior displays include optical clarity, scratch resistance, impact resistance, temperature resistance, anti-glare properties, touch screen compatibility, UV protection, easy to clean. Due to enhanced strength, durability, and safety characteristics chemically strengthened glass is typically used as the cover glass for in-vehicle displays (for instance, AutoGrade™ Corning® Gorilla® Glass, see Corning Inc. (2025)).

The headform impact test is required by the automotive industry to assess the display's ability to withstand impact forces and protect occupants from injury in the event of a crash. During the test, a specially designed headform, representing the head of an occupant, is propelled towards the display at a specified speed and angle to simulate a potential impact during a crash. The impact velocity is determined based on regulatory standards or industry guidelines to simulate realistic crash scenarios. The performance of the display is evaluated based on criteria such as deflection, deformation, and damage. The display should be able to absorb the impact energy and prevent sharp or hazardous fragments from breaking off. To ensure occupant safety during impact the criteria for headform deceleration is used. The deceleration of the headform refers to how quickly the headform comes to a stop upon impact with the display. The deceleration criteria are defined based on industry standards, regulations, or specific performance requirements. The maximum allowable deceleration level is often specified in terms of g-forces, where 1 g represents the acceleration due to gravity 9.81 m/s^2. The deceleration level is typically limited to certain values to prevent excessive forces on the headform and reduce the risk of head injuries. In addition to the maximum deceleration level, the duration of the deceleration is also considered in the criteria. Rapid deceleration over a short duration can increase the risk of injury, so there may be requirements for the deceleration to occur gradually or within a specified time frame.

The headform impact test procedure is defined by government regulations such as FMVSS201 in the USA, GB 11552 in China and ECE R21 in the EU/UN. There are some differences in the test conditions and the system performance requirements, but the general requirement that is difficult to meet is that the total headform deceleration must not exceed 80g for more than 3ms. The most common way to improve the test performance is to use a soft material for display support structure that smoothly absorbs the kinetic energy of the headform. This method has an important limitation: on the one hand, the softer the material, the better the performance, but on the other hand, very soft material leads to a significant increase in deformation, even with touch screen use.

To overcome this challenge, we propose to use a display support structure that exhibits temporary and reversible loss of shape stability under the head impact loading conditions. This structure allows to reduce headform deceleration to be within required level and reduces stress in the cover glass to improve its survivability in the head impact test. This benefit applies to head impacts over the surface of the display module as well as near the edge of the glass, helping to improve the edge strength problem which is hard to improve otherwise. The main advantage of the proposed structure is that it improves the headform impact test performance without losing screen functionality. I.e., the display support is still stiff for its regular use but is capable to smoothly absorb the kinetic energy of the headform.

2. Display support with bilinear response - Simplified 1D analysis

This section aims to illustrate the principal idea of the support with bilinear response. Here we use very simplified model to focus on the based effect. The model consists of a mass m and a spring c. The mass simulates the headform, while the spring simulates the display module with the support structure. Suppose that the elastic force due to spring compression obeys Hook's low. Then if y is the spring compression, Newton's second law gives the following equation:

$$m\ddot{y} + cy = 0 \tag{1}$$

The initial conditions are (just before impact of the headform with the display module)

$$y(0) = 0$$
$$\dot{y}(0) = \dot{y}_0 \tag{2}$$

The solution of the equation (1) with the initial conditions (2) is well-known and has the following form

$$y(t) = \frac{v_0}{\omega}\sin(\omega t) \tag{3}$$

The compression force (or contact force between the headform and the display) is

$$F = cy = c\frac{v_0}{\omega}\sin(\omega t) \tag{4}$$

The force reaches its maximum when $\sin(\omega t) = 1$ or $t = \frac{\pi}{2\omega}$.

$$F_{max} = c\frac{v_0}{\omega} = v_0\sqrt{cm} \tag{5}$$

Deceleration is proportional to the contact force

$$a_{max} = \frac{F_{max}}{m} = v_0\sqrt{c/m} \tag{6}$$

The headform initial speed and its mass are specified by the normative documents. This means that the level of deceleration can be controlled only by the display stiffness including the support structure (for simplicity further we will refer to this stiffness as "support stiffness").

From this simplified model we can say that the deceleration is proportional to the square root of the support stiffness and if we want to decrease the deceleration, we need decrease the support stiffness. Of course, in the application we have limitation for the display stiffness: it cannot be too small. For instance, the compression cannot be greater than the dashboard width. I.e. there is the following limitation for the spring compression

$$y_{max} = \frac{v_0}{\omega} = \frac{v_0\sqrt{m}}{\sqrt{c}} \le h, \tag{7}$$

where h is the top bound of the spring compression. From this equation one can get the limitation for the spring stiffness

$$c \ge \frac{v_0^2 m}{h^2}. \tag{8}$$

It should be noted that this limit satisfies energy balance: the whole amount of initial kinetic energy transfers to elastic energy of the spring (we will use it below):

$$\frac{cy_{max}^2}{2} = \frac{ch^2}{2} = \frac{v_0^2 m}{h^2}\frac{h^2}{2} = \frac{v_0^2 m}{2}. \tag{9}$$

This spring stiffness produces the following bottom bound of the maximum deceleration

$$a_{max} \geq \frac{v_0^2}{h}. \tag{10}$$

Thus, the optimal spring stiffness providing minimum deceleration level (10) is expressed by equation (8).

Next, suppose that the elastic force depends on the spring compression in the way shown in Fig. 1. I.e. the spring stiffness equals to

$$c(y) = \begin{cases} c_1, & y < y_1 \\ c_2, & y \geq y_1 \end{cases} \tag{11}$$

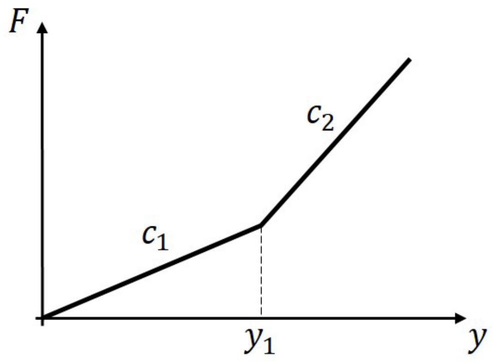

Fig. 1: Bilinear response of the support structure.

For $y < y_1$, the problem is similar to the one considered above and the compression is

$$y(t) = \frac{v_0}{\omega_1}\sin(\omega_1 t), \tag{12}$$

where

$$\omega_1 = \sqrt{\frac{c_1}{m}}$$

The elastic force is

$$F_1(y) = c_1 y \tag{13}$$

For $y > y_1$, the elastic force equals to

$$F_2(y) = c_2 y + (c_1 - c_2)y_1 \tag{14}$$

Then the differential equation of motion is

$$m\ddot{y}(t) + c_2 y(t) + (c_1 - c_2)y_1 = 0 \tag{15}$$

To start time counting from zero, we will introduce the new time variable

$$\tilde{t} = t - t_1 \tag{16}$$

Let us reduce this problem to the previous one by introducing the new variable $\tilde{y}(\tilde{t})$:

$$F_2 = c_2\left(y(t) + \left(\frac{c_1}{c_2} - 1\right)y_1\right) = c_2\tilde{y}(\tilde{t}), \tag{17}$$

where

$$\tilde{y}(\tilde{t}) = y(\tilde{t} + t_1) + \left(\frac{c_1}{c_2} - 1\right)y_1.$$

Since that, the differential equation of motion is as previously

$$m\ddot{\tilde{y}}(\tilde{t}) + c_2\tilde{y}(\tilde{t}) = 0 \tag{18}$$

We will name the solution of the previous stage (when $y < y_1$) by $y_{prev}(t)$. Then the initial conditions for equation (18) are

$$\tilde{y}(0) = \frac{c_1}{c_2}y_{prev}(t_1)$$
$$\dot{\tilde{y}}(0) = \dot{y}_{prev}(t_1) \tag{19}$$

The solution of (18) is

$$\tilde{y}(\tilde{t}) = A\sin(\omega_2\tilde{t} + \varphi), \tag{20}$$

where

$$\omega_2 = \sqrt{\frac{c_2}{m}}. \tag{21}$$

Using the initial conditions (19), one can get:

$$\begin{cases} A = \sqrt{\left(\frac{c_1}{c_2}y_{prev}(t_1)\right)^2 + \left(\frac{\dot{y}_{prev}(t_1)}{\omega_2}\right)^2} \\ \varphi = \operatorname{atan}\frac{c_1\omega_2 y_{prev}(t_1)}{c_2\dot{y}_{prev}(t_1)} \end{cases}. \tag{22}$$

Thus, returning to the former variables, we have the following solution

$$y(t) = A\sin(\omega_2(t - t_1) + \varphi) - \left(\frac{c_1}{c_2} - 1\right)y_1. \tag{23}$$

The contact force is

$$F_{contact} = c_2 y(t) + (c_1 - c_2)y_1. \tag{24}$$

The contact force reaches its maximum when

$$\sin\left(\omega_2(t - t_1) + \operatorname{atan}\frac{c_1\omega_2 y_1}{c_2\dot{y}_1}\right) = 1, \tag{25}$$

or

$$(t - t_1) = \frac{1}{\omega_2}\left(\frac{\pi}{2} - \operatorname{atan}\frac{c_1\omega_2 y_1}{c_2\dot{y}_1}\right), \tag{26}$$

and equals to

$$F_{contact_{max}} = c_2\sqrt{\left(\frac{c_1}{c_2}y_1\right)^2 + \left(\frac{\dot{y}_1}{\omega_2}\right)^2}. \tag{27}$$

Corresponding maximum deceleration is

$$a_{max} = \frac{F_{contact_{max}}}{m} = \frac{c_2}{m}\sqrt{\left(\frac{c_1}{c_2}y_1\right)^2 + \left(\frac{\dot{y}_1}{\omega_2}\right)^2}. \tag{28}$$

The result is not so trivial as for the linear spring and it provides more opportunities for the support structure optimization. To analyse the result let us rewrite expression for the maximum deceleration (28). As previously, we assume that spring compression is limited by h and to find the optimal stiffnesses (c_1 and c_2) we use the following limitation

$$y_{max} = h. \tag{29}$$

Further, we introduce the new dimensionless variables

$$\alpha = c_1/c_2, \tag{30}$$

$$\beta = y_1/h. \tag{31}$$

It should be noted that $\beta \leq 1$, while $\alpha > 0$.

Then equation (24) at $y = h$ takes the form

$$F_{contact} = c_2 h + (c_1 - c_2)y_1 = c_2 h(1 + (\alpha - 1)\beta) \tag{32}$$

Energy balance provides us the following equation

$$\frac{mv_0^2}{2} = \frac{c_1 y_1^2}{2} + \frac{1}{2}(F_{max} + c_1 y_1)(h - y_1) \tag{33}$$

Right hand side of this equation is the area under lines shown in Fig. 1. Using (32) and dimensionless variables (30-31) one can rewrite equation (33) in a following form

$$\frac{mv_0^2}{c_2 h^2} = 1 - \beta(2 - \beta)(1 - \alpha). \tag{34}$$

or

$$c_2 h = \frac{mv_0^2}{h}\frac{1}{1 - \beta(2 - \beta)(1 - \alpha)}. \tag{35}$$

And then expression for the maximum contact force (32) takes the following form

$$F_{max}(\alpha, \beta) = \frac{mv_0^2}{h}\frac{1 + (\alpha - 1)\beta}{1 - \beta(2 - \beta)(1 - \alpha)} \tag{36}$$

For the maximum deceleration we have, respectively,

$$a_{max}(\alpha,\beta) = \frac{F_{contact_{max}}(\alpha,\beta)}{m} = \frac{v_0^2}{h}\frac{1+(\alpha-1)\beta}{1-\beta(2-\beta)(1-\alpha)} \tag{37}$$

We are interested in comparing of the bilinear spring with the linear one. It should be noted that the linear spring is a particular case for the bilinear at $\alpha = 1$. For the further analysis we use the dimensionless deceleration

$$f_{max}(\alpha,\beta) = \frac{a_{max}(\alpha,\beta)}{\frac{v_0^2}{h}} = \frac{1+(\alpha-1)\beta}{1-\beta(2-\beta)(1-\alpha)} \tag{38}$$

Note that for the linear spring the dimensionless deceleration is equal to 1. The dimensionless deceleration vs stiffness ratio (α) are sown in Fig. 2. The most important conclusion is that for $\alpha < 1$ ($c_1 < c_2$) the dimensionless deceleration is large than 1, while for $\alpha > 1$ ($c_1 > c_2$) the dimensionless deceleration is lower than 1. This means that a “softer” ($c_1 < c_2$) contact start will result in a higher contact force, while a “harder” contact start will result in a lower contact force. Below we will provide physical explanation of this effect. From Fig. 2 we also see that the dimensionless deceleration is monotonic with respect to the stiffness ratio: the higher the stiffness ratio the lower the dimensionless deceleration. This immediately follows from the first derivation of (38) with respect to α:

$$\frac{\partial f_{max}(\alpha,\beta)}{\partial\alpha} = -\frac{\beta(1-\beta)}{\left(1+\beta(2-\beta)(\alpha-1)\right)^2} \tag{39}$$

i.e. the first derivation is a nonpositive function (as $0 \le \beta \le 1$). Meanwhile the dimensionless deceleration is nonmonotonic with respect to dimensionless stiffness change β: for $\alpha < 1$ there is the maximum of the dimensionless contact force and for $\alpha > 1$ there is the minimum of the dimensionless deceleration.

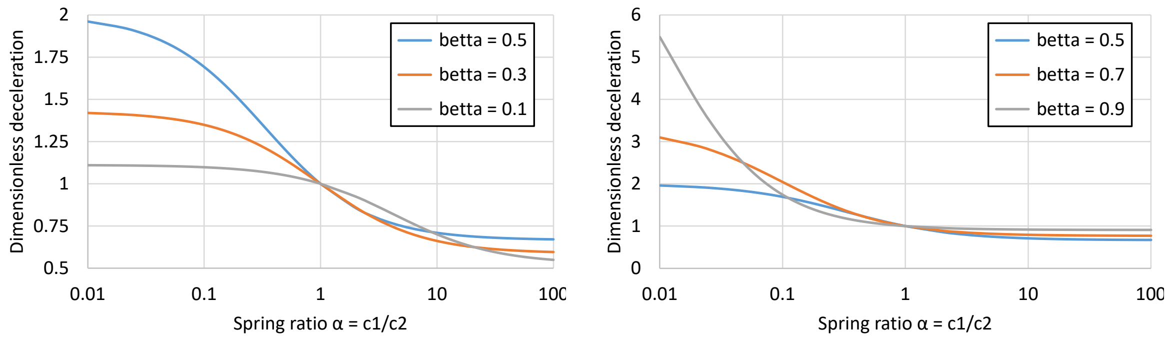

a) $\beta \le 0.5$ b) $\beta \ge 0.5$

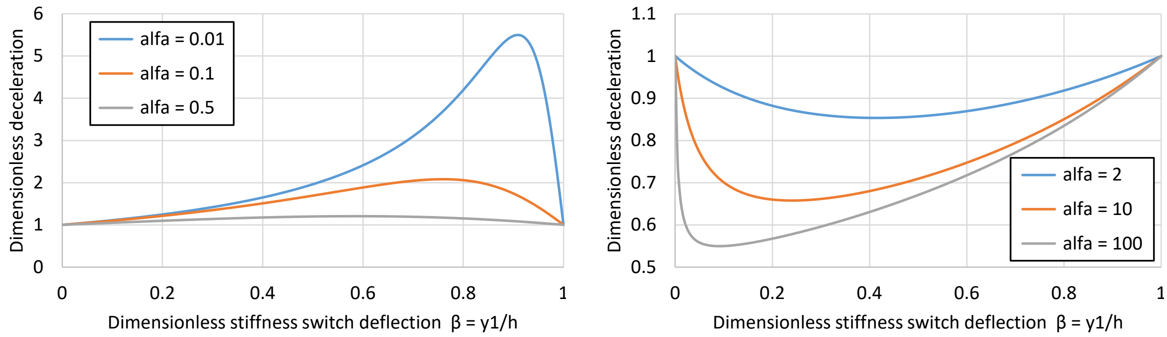

c) $\alpha < 1$ d) $\alpha > 1$

Fig. 2: Dimensionless deceleration as function of system parameters.

Fig. 3 provides a simple explanation of the effect on deceleration (or contact force, as they are proportional) at different parameters of the bilinear function. Due to energy conservation low the whole amount of kinetic energy just before the impact transfers into strain energy in the spring. The strain energy is an area under “Force-Spring compression” plot. For the linear spring this is the area of the triangle. A softer spring for a small compression ($y < y_1$) results in smaller area at the beginning, i.e. a smaller amount of kinetic energy transfers to the spring energy and to be able to accumulate the rest of the kinetic energy in the second part of the process ($y > y_1$) maximum force must reach a higher magnitude. On the contrary, a stiffer spring for small compression ($y < y_1$) results in the accumulation of greater amount of kinetic energy and, therefore, to be able to accumulate the rest of the kinetic in the second part of the process ($y > y_1$) the maximum force reaches a lower magnitude. Obviously, for both cases with the bilinear springs shown in Fig. 3 the total area is the same, i.e. the areas of the green and blue triangles are the same. The optimal bilinear response “transfers” the triangular shape of the linear response to the rectangular shape of the bilinear response when the stiffness ratio α tends to infinity and the stiffness change β tends to zero. In this case, the maximum contact force is two times lower than for the linear response.

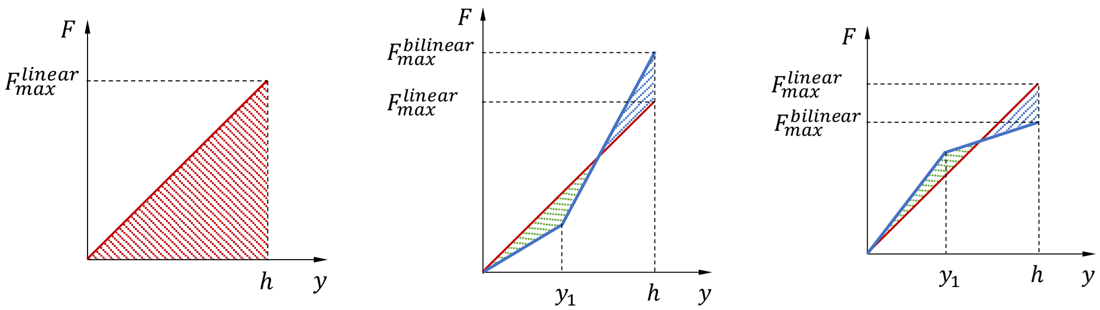

a) linear spring

b) bilinear spring with soft entrance

c) bilinear spring with hard entrance

Fig. 3: Illustration of the bilinear stiffness benefit in the case of hard entrance.

In summary of this section, we have shown that bilinear spring response can significantly reduce the magnitude of deceleration. In limiting case the magnitude can be reduced by a factor of two compared to the linear response for the same compression. This provides an opportunity to optimize the display support structure making the system more reliable. Equation (37) provides a guide to finding the optimum parameters for the bilinear response: (a) the stiffness should be high at the beginning of the impact and then low; (b) the ratio of the stiffness should be as high as it possible. There are several ways in which this type of response can be achieved. For instance, elastic material response with a subsequent plastic zone (e.g. Badar et al (2021)) or hyperplastic behaviour of rubber-like material. Another possibility which we will be considered further, is a structural response with buckling. There are many possible realizations of buckling structure, for example honeycomb or beam types of structure, which are analysed in detail by Gibson and Ashby (1997). One of the additional advantage of such a structure is that there is no permanent deformation during loading, which avoids the need to rebuild the structure after the impact.

3. Display support with bilinear response – Full-scale 3D analysis

This section aims to illustrate the efficiency of the proposed display support structure design using a realistic 3D model. The mechanical response of the display is very complex, involving system level vehicle architecture such as the instrument panel, vehicle cross beam, etc (see e.g. Keranen et al (2005) and Malladi, Saifuddin, and Gadekar (2011)). In order to make a general assessment of the display's performance, a simplified model is used in this section, see Fig. 4. We assume that the display module consists of 3 layers: glass, adhesive, and aluminium plate with thicknesses of 1.1 mm, 0.2 mm, and 2 mm, respectively. The width and length of the display module are 117.9 and 308.4 mm respectively. The headform impactor is modelled as a half of rigid sphere with radius of 82.5 mm and a mass of 6.8 kg, possessing a resulting kinetic energy at impact of 152J. The support structure is simulated by 1D linear elements distributed along two edges of the display, in five rows per edge with 21 elements per row.

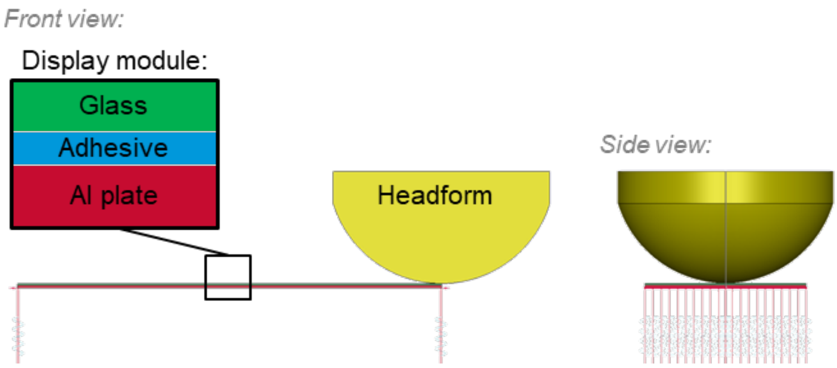

Fig. 4: The FEA model.

For the baseline case the support structure is represented by linear springs with a stiffness c of 0.25 N/mm following to the concept introduced by Layouni et al (2017). To evaluate performance of the proposed support structure with buckling we use springs with the bilinear stiffness. The schematic representation of linear and bilinear stiffnesses of springs is shown in Fig. 5. The stiffness c_1 and c_2 are related to the linear stiffness c with coefficient k through equations (40) and (41). To compare the bilinear response the k coefficients of 8 and 10 are utilized. The stiffness changes at compression of 1.5 mm for both cases. The material properties of model parts are listed in Table 1.

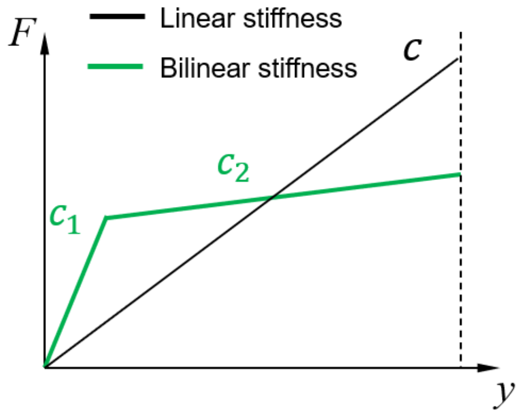

Fig. 5: Schematic representation of linear and bilinear stiffnesses of springs.

$$c_1 = k \cdot c, \tag{40}$$

$$c_2 = c/k. \tag{41}$$

Table 1: Mechanical properties of the model parts.

Part	Material	Density [kg/m ^{3}]	Young's Modulus [MPa]	Poisson's Ratio
Cover glass	Autograde glass	2430	76700	0.21
Adhesive	Adhesive	1300	5	0.47
Plate	Al 6061	2700	69000	0.33

Dynamic finite element analysis is carried out using LS-DYNA explicit solver. The impact position is nearby glass edge as the most critical one. The simulation starts from the moment when the impactor touches the display and the specified in standard initial velocity is set. The results after applying a Butterworth filter to remove numerical noise are shown in Fig. 6. The baseline case is chosen so that it does not meet the requirement for the headform deceleration: the deceleration exceeds the top limit of 80 m/s^2 for more than 3 ms, see Fig. 6, a. As can be seen from Fig. 6, a, the deceleration magnitude for the bilinear stiffness of the support structure is reduced by 33-42% compared to the baseline case and meets the requirement. The peak stress in the cover glass is reduced by 8 %, see Fig. 6, b, making the display more reliable. At the same time, as it is shown in Fig. 6, c, the total deflection of the display at the point of contact is almost the same as for the baseline case. The concept therefore facilitates the reduction of headform deceleration to meet industry standards, decreases stress in the cover glass to enhance display reliability, all while maintaining the overall deformation of the display.

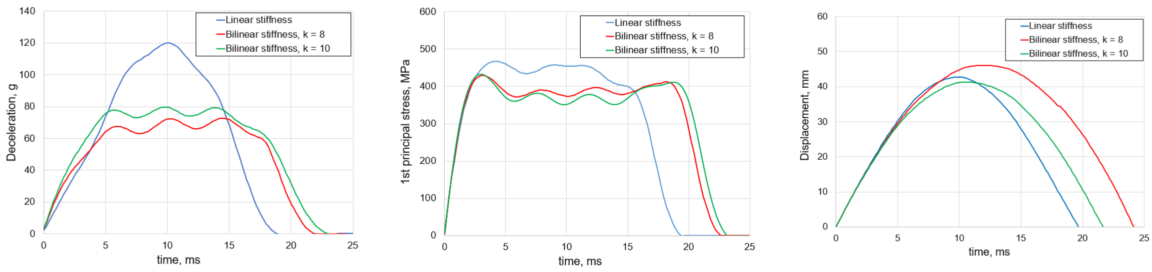

a) *b)* *c)*

Fig. 6: Finite element simulation results: a) Deceleration of the headform; b) Max 1st principal stress in the cover glass; c) Impactor displacement.

4. Conclusions

In this study we demonstrated that implementing a bilinear response for the display support structure can lead to a significant reduction in deceleration magnitude during impacts. The study has revealed that under certain conditions, the magnitude of deceleration can be halved compared to a linear response for the same compression, offering an opportunity to enhance the reliability of the system. Simplified analytical analysis made in the study provides the insight to specify bilinear response parameters for a particular display module and vehicle to satisfy requirements for the headform impact test. To realize bilinear response, we propose to use buckling structure to avoid permanent deformation making possible reuse of the structure after impact event without repair the support structure. Using 3D finite element approach, we confirmed the conclusion of the simplified analytical analysis and also showed that the concept with bilinear stiffness allows to reduce stress in cover glass improving reliability of the display module.

References

Badar A.G., Layouni K., Park J.S., Qaroush Y.K., Yang Y. (2021) High-impact energy absorption connection design for auto interior display module under head form impact. US Patent Application 20210354645A1

Corning Inc. (2025) Interior Automotive Glass. Corning Inc. https://www.corning.com/gorillaglass/worldwide/en/applications/automotive/dashboards_consoles.html

Gibson L., & Ashby M. (1997). Cellular Solids: Structure and Properties (2nd ed.). Cambridge Solid State Science Series. Cambridge: Cambridge University Press. doi: http://doi.org/10.1017/CBO9781139878326

Keranen M., Krishnaraj S., Kulkarni K., Lu L., Thyagarajan R., Ganesan V. "Automating Instrument Panel Head Impact Simulation," SAE Technical Paper 2005-01-1221, 2005, https://doi.org/10.4271/2005-01-1221

Layouni K., Gross T.M., Black M.L., Harris J.T., Park J.S., Qaroush Y.K. (2019) Retained Strength for AutoGrade™ Cover Glass. Retrieved from https://www.corning.com/microsites/ags/downloads/white-papers/retained-strength-for-autograde-cover-glass-whitepaper.pdf

Malladi A., Saifuddin, and Gadekar G. "CAE Based Dashboard Development for Head form Impact Test as per IS15223 and ECE R21 Requirements," SAE Technical Paper 2011-26-0014, 2011, https://doi.org/10.4271/2011-26-0014